

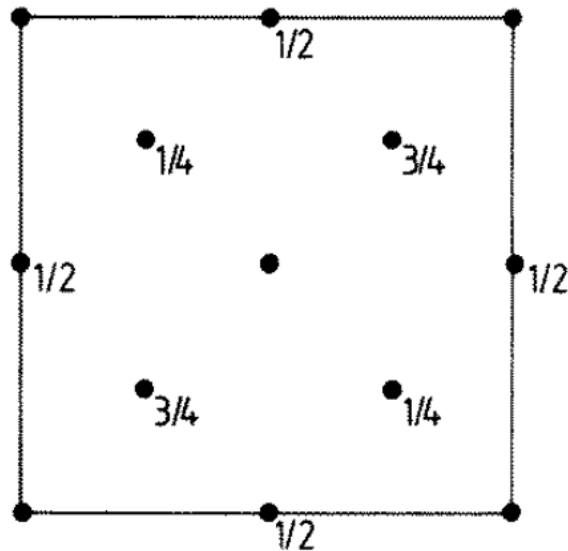
# MASTER OF PHILOSOPHY Modelling of Materials

## Examiners' Solutions to Paper 1

### SECTION A

1(a)

There are four lattice points in the cell, and hence eight carbon atoms per unit cell.



1(b)

Explanation depends on the result that the number of allowed wave vectors in a band equals  $N$ , the number of primitive cells in the crystal. Extra credit should be given if this result is proved.

[Proof: From free electron theory, the allowed wave vectors in a 1-D box of length  $L$  is given by

$$k = \frac{2\pi n}{L} = 0, \pm \frac{2\pi}{L}, \pm \frac{4\pi}{L}, \dots, \pm \frac{2\pi n}{L} \quad \text{where } n \text{ is integer.}$$

*i.e.* the number of allowed wave vectors is equal to  $2n$ .

Within the first band, the series terminates at  $\pm \frac{\pi}{a}$ , where  $a$  is the lattice parameter. Therefore  $\pm \frac{2\pi n}{L} = \pm \frac{\pi}{a}$ . But  $Na = L$ , where  $N$  is the number of primitive cells in the crystal, and thus  $2n = N$ . Hence the number of allowed wave vectors is equal to  $N$ ]

Taking into account the Pauli exclusion principle which says that 2 electrons can occupy each  $k$ -state, then there are  $2N$  allowed electrons per band (an even number). Therefore crystals with an even number of valence electrons per primitive cell will have full bands. A crystal with full bands will be an insulator since an external electric field will not cause current to flow. Provided that there is an energy gap, there is no continuous way to change the momentum of the electrons if every accessible state is filled. Extra credit should be given if it is recognized that there are exceptions to this rule when there is band overlap.

Crystals with an odd number of electrons per primitive cell will have half filled bands. There are therefore accessible states to facilitate conduction and the crystal is a metal. Examples: Na that has 1 electron per primitive cell and is a metal. Si that has 8 electrons per primitive cell is an insulator (at zero Kelvin). Simple sketches of how the electrons occupy the levels in the band are appropriate.

1(c)

A multiscale model couples different models across the length scales. A good answer will define the hierarchy of models based on length scale (*i.e.* electronic, atomistic, microstructural and continuum) and note that the main idea is to integrate two or more of them. Sketches of length scale against discipline or length scale against number of atoms would be appropriate. Additional credit could be given for pointing out that models on individual length scales are now well established and that multiscale modelling is the current challenge in modelling research (the intermediate scale problem).

Any example where it would be computationally advantageous to model different behaviour on different length scales simultaneously would suffice. Example given in lectures was fracture where the tip of the crack is modelled atomistically and the long-range strain field is modelled elastically. The scale of the models have to be chosen appropriately to target the main process that is occurring, e.g. bond breaking or bond

stretching. The main idea is to avoid doing detailed microscopic or microstructural calculations in regions of the model where it is unnecessary, and to account for long-range behaviour with macroscopic solutions. The main technical difficulty is making sure that the solutions are continuous across the boundaries between different models.

1(d)

A process whose direction can be changed by an infinitesimal alteration in the external conditions is called *reversible* (for example, a frictionless piston compressing an ideal gas in a cylinder). By contrast, free energy is dissipated in an irreversible process.

A *steady-state process* is one in which free energy is being dissipated but it is possible to define a frame of reference such that the process appears stationary. For example, in steady-state diffusion, free energy is being dissipated but the concentration profile does not change.

The flux may be written as a function  $J\{X\}$  of the force  $X$  using a Taylor expansion about  $X = 0$

$$J\{X\} = J\{0\} + J'\{0\} \frac{X}{1!} + J''\{0\} \frac{X^2}{2!} + \dots$$

Note that  $J\{0\} = 0$  since the flux is zero at equilibrium. If the high order terms are neglected, then we see that  $J \propto X$ .

1(e)

---

```

subroutine tform (t, l, tprime)
implicit none
integer alpha, beta, i, j
real t(3,3), l(3,3), tprime(3,3)
do 20, alpha = 1, 3
do 20, beta = 1, 3
tprime(alpha, beta) = 0.0
do 10, i = 1, 3
do 10, j = 1, 3
tprime(alpha, beta) = tprime(alpha, beta) + l(alpha, i) *
$      l(beta, j) * t(i,j)
10 continue
20 continue
return
end

```

1(f)

The principal differences are that metallic melts are much higher temperature and lower viscosity than polymer melts, and consequently the stresses applied to the mould during injection moulding are much higher than during casting. This necessitates having an extremely durable mould with a smooth surface finish. Also, the thermal diffusivity of metals is much higher than that of most polymers, and so the cooling phase is generally faster for metal casting. Heat conduction from the mould is a particular issue for thermoplastic polymers, which do not obtain sufficient dimensional stability to retain their moulded shape until they are well below the melting temperature. Thus, mould designs for injection-moulded polymer components tend to avoid containing large contiguous blocks of polymer wherever possible. They also tend to avoid having sharp corners or narrow channels in which shear-orientation of the polymer chains can occur, causing anisotropic swelling and shrinkage during cooling.

1(g)

The SHAKE algorithm can be used to freeze any set of holonomic constraints (bond length, bond angle, torsion angle) during a molecular dynamics simulation. However, it cannot be used to enforce non-holonomic constraints (*i.e.* those which are not a function of the atomic coordinates). The method works by introducing fictitious constraint forces that act along the bond vectors between each pair of atoms. In the case of a diatomic, there are two equal and opposite forces acting along a vector connecting the atoms.

The magnitudes of the forces are determined by substituting the standard forces (calculated from derivative of potential energy) plus constraint forces into the discretised equations of motion for the MD simulation, and imposing the constraint that  $|\mathbf{r}_{ij}(t + \Delta t)| = |\mathbf{r}_{ij}(t)| = d_{ij}$ , where  $r_{ij}$  are the positions of the atoms at adjacent points in the trajectory, and  $d_{ij}$  are the bond lengths to be enforced. This leads to a set of simultaneous equations that can be recast into a matrix form and solved by inverting the matrix.

For larger molecules, this is very time consuming and so an iterative procedure is used (hence the “shaking” of the molecule as each constraint is enforced in turn).

1(h)

Both Brownian dynamics and DPD, are based on a simple molecular dynamics type approach except that in addition is a random ‘kick’ term and a dissipative term, in which the energy injected by the ‘kick’ is drained away between the events by a damping term proportional to particle velocity.

However, in the case of Brownian Dynamics both terms act in relation to the rest frame of the simulation, so simulations are diffusive rather than hydrodynamic. In the case of DPD, the same forces (random kick and damping) are present, but they are applied to the interaction between particles and thus there is proper conservation of both linear and angular momentum.

DPD can be applied to model short, diblock copolymers by building mesoscopic models for the diblocks from DPD beads (each containing many atomistic particles) and mapping the conservative interaction parameters between the beads onto standard Flory-Huggins theory for the homopolymer case.

1(i)

In the phase-field method, the state of the entire microstructure is represented continuously by a single variable known as the *order parameter*  $\phi$ . For example,  $\phi = 1$ ,  $\phi = 0$  and  $0 < \phi < 1$  represent the precipitate, matrix and interface respectively. The latter is therefore located by the region over which  $\phi$  changes from its precipitate-value to its matrix-value. The range over which it changes is called the *width* of the interface. The set of values of the order parameter over the whole microstructure is the *phase field*.

The term  $\varepsilon(\nabla\phi)^2$  represents the free energy component due to the heterogeneous nature of the system, where the order parameter is not constant. It can be regarded as an interfacial energy, although the interface may be broad.

1(j)

Interfacial stability during growth determines whether the transformation occurs at a dendritic, cellular or planar front. The stability of the interface

to perturbations depends on the nature and extent of the undercooling beyond the interface (*e.g.* thermal and solute gradients).

Strain energy due to transformation affects the shape as the precipitate attempts to minimise strains. In the case of martensitic transformation this leads to a thin-plate shape.

The minimisation of interfacial energy can determine the equilibrium shape. The shape will be spherical when the interfacial energy does not depend on orientation. More complex equilibrium shapes are found when the latter is not true.

## SECTION B

2.

A neural network is a very flexible, non-linear function that can capture complex patterns in data, whereas a linear regression method begins with the assumption that the problem is linear. Because of this flexibility, it is also able to represent better the interactions between input variables. With a neural network it is not necessary to specify the functional relation between the input and output variables at the beginning of the analysis.

[20%]

The experimental data are randomly divided into training and test data. The former is used to create the model, and the latter to assess its ability to generalise. One way to avoid overfitting is to minimise the test error resulting from fitting to the training data. Whilst the error resulting from the training data will be a monotonically decreasing function of the number of training steps, the test error will have a minimum at the point where overfitting begins to occur.

[25%]

Fewer data will lead to a greater uncertainty of modelling, since many functions can in principle fit the same data.

[15%]

The greater the level of noise in the experimental data (*e.g.* when repeated experiments give different results), the worse will be the ability to create a good model. Similarly, mistakes made in assembling the dataset will lead to outliers that can skew the training process. The data may not be uniformly dispersed in the input space, in which case the predictions may be uncertain in the regions where data are sparse.

[30%]

Input data with the highest significance for predicting the strength of a steel weld include: ultimate tensile strength, yield strength, tempering time, tempering temperature, heat input, oxygen content and chemical composition. The majority of these factors should be given for full credit.

[10%]

3.

Hardening (increase in plastic yield stress) is clearly of interest for structural materials. It is particularly useful for the lightweight metal aluminium that cannot be hardened by the types of polymorphic transformation (austenite-ferrite) applicable in steels. Choice of the annealing treatment allows fine control of the mechanical properties, including a compromise between hardness (high yield stress) and ductility.

[10%]

The yield stress is an extrinsic property, strongly affected by the microstructure of the material. In contrast, Young's modulus is an intrinsic property largely independent of microstructure and dependent on the average bonding in the material. Young's modulus is affected very little by precipitation. Electron scattering by solute atoms is much stronger than by particles. As the copper atoms in solution in the aluminium matrix in Al-Cu come out of solution and form precipitates (of  $\text{Al}_2\text{Cu}$ ), the electrical resistivity falls.

[20%]

The maximum in yield stress is observed on annealing an Al-Cu alloy in which all the copper is initially in solid solution in the aluminium. (This supersaturated state is achieved by quenching after a solution treatment at high temperature — this might be illustrated on a phase diagram, but this is not an essential part of the answer.) Plastic flow is by dislocation motion, and this is impeded by the formation of precipitate particles. In the early stages of annealing the supersaturated solid solution, the precipitates are fine and their overall volume fraction increases with time. In this regime the dislocations cut through the precipitate particles and this cutting becomes more and more difficult. In the later stages of the annealing, the precipitation is complete (the final volume fraction is reached), but the particles undergo Ostwald ripening. The precipitate dispersion coarsens to give fewer, larger particles, a change favoured by the reduction of particle-matrix interfacial area. In the coarsened dispersion, the inter-particle separation increases, and the dislocations can bow between the particles with increasing ease.

[40%]

The last part of the question is deliberately open-ended, designed to permit a wide range of answers that might include some of the following:

— One possibility is to eschew mechanistic analysis and to use neural-network modelling: accumulated hardening data can then contribute to a quantitative model.

- Another possibility is to focus on the need to model transformation kinetics, using the Avrami approach for fraction precipitated and the basic laws for Ostwald ripening.
- More detailed modelling could tackle the nucleation and growth of the precipitate particles.
- There may also be interest in modelling the dislocation dynamics.
- Thermodynamic modelling can be used for phase-diagram prediction, important for predicting precipitate phase, composition and equilibrium volume fraction.
  - Diffusion modelling may be important in understanding initial formation of a uniform-composition supersaturated solid solution, as well as providing an underpinning for the microstructural modelling.

[30%]

4.

The main parameters for analysis of a 2-D heat transfer problem are the intrinsic material properties (*e.g.* thermal conductivity of the constituent materials) and the boundary conditions (convection, conduction, radiation, heat generation or input, etc.) Since no large-scale deformation is being considered, we do not need to be concerned about distortion of the elements and remeshing. To minimise the number of nodes and decrease computation time, a simple three-node triangular element should be used for the problem described in the question.

[25%]

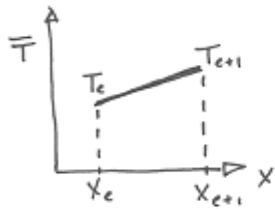
For problems involving large-scale deformation, constitutive relationships describing stress, strain, strain rate, etc. are required, along with the usual parameters required for heat transfer problems. Additionally, assumptions regarding the nature of elastic deformation (rigid, perfectly elastic, elastic-plastic, elastic-perfectly plastic) need to be addressed in the FE analysis. Due to large-scale deformation, nodal positions become displaced and the elements must be able to undergo remeshing. Elements suitable for remeshing are the three node triangular element and the two dimensional mini element.

[25%]

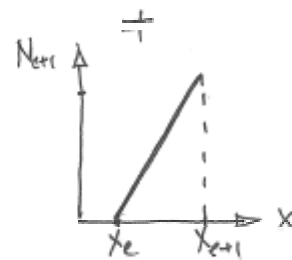
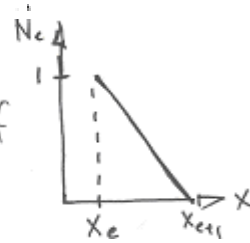
Shape functions are comprised of a linear combination of functions that relate the numerical nodal values to the function values and approximate the exact solution within the element (see diagram below). Between adjacent nodes, the shape function expresses the particular set of partial differential equations as integrals or averages of the solution. Shape functions can be quadratic or linear. Essentially, shape functions

distinguish the finite element method from other simpler analysis techniques such as the finite difference method.

c) Linear Shape functions

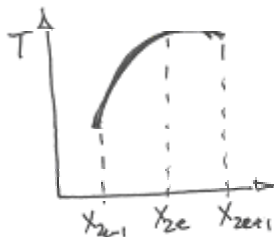


is a combination of

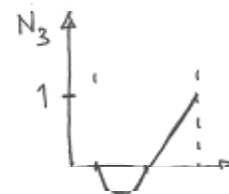
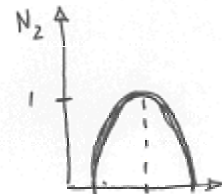
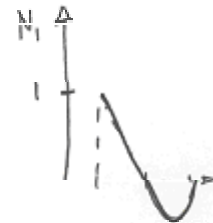


OR

Quadratic Shape functions



is a combination of



[40%]

Experimental validation is required to obtain the actual solution to the Jominy end quench bar problem.

[10%]

5.

Partition function  $Z = \sum_i \exp(-E_i / k_B T)$ , or alternatively

$Z = \sum_i \exp(-\beta E_i)$ , where  $\beta = 1/(k_B T)$  and  $E_i$  are the energies of each microstate  $i$ . In each case, the sum runs over all microstates of system.

Helmholtz free energy  $F = -k_B T \ln Z$ .

[A derivation is not required, but follows simply from the above definition of partition function if enthalpy is substituted for energy]

[20%]

For a single particle:

$$\begin{aligned} Z_1 &= 1 + \exp(-V\varepsilon / k_B T) + \exp(V\varepsilon / k_B T) \\ &= 1 + 2 \cosh(V\varepsilon / k_B T) \end{aligned}$$

Hence for  $N$  independent, distinguishable particles:

$$Z_N = [1 + 2 \cosh(V\varepsilon / k_B T)]^N$$

$$dF = -SdT - pdV$$

$$\therefore p = -\left(\frac{\partial F}{\partial V}\right)_T = \frac{\partial}{\partial V} \left\{ Nk_B T \ln [1 + 2 \cosh(V\varepsilon / k_B T)] \right\}$$

$$\Rightarrow p = \frac{2N\varepsilon \sinh(V\varepsilon / k_B T)}{1 + 2 \cosh(V\varepsilon / k_B T)}$$

[50%]

If particles are not independent, then partition function will not factorise and the analytical derivative of the Helmholtz free energy will become extremely unwieldy to compute. An alternative is to use either Metropolis Monte Carlo (constant volume) to calculate the system pressure as a function of volume, or isothermal-isobaric Monte Carlo (constant pressure) to calculate system volume as a function of pressure. A brief summary of the general Monte Carlo algorithm should be given, including volume-changing moves for constant pressure method.

[30%]

6.

Growth is said to be diffusion-controlled when the majority of the free energy available is dissipated in the diffusion of solute ahead of the interface. Interface-controlled growth is said to occur when the majority of the free energy is dissipated in the transfer of atoms across the boundary.

[20%]

Calculate independently, the growth rate using the diffusion-controlled growth equation as a function of free energy. Similarly calculate the growth rate using the interface-controlled growth equation as a function of free energy. There is only one interface; both equations must therefore give the same velocity. The respective dissipations must therefore be chosen such that the velocity obtained from each function is the same. The students may use the electrical analogy (lecture notes) to explain this.

[20%]

The volume of a particle nucleated at time  $t = \tau$  is given by

$$v_\tau = \frac{4}{3}\pi G^3 (t - \tau)^3$$

The change in extended volume over the interval  $\tau$  and  $\tau + d\tau$  is

$$dV_e^\alpha = \frac{4}{3}\pi G^3 (t - \tau)^3 \times I_V \times V \times d\tau$$

On substituting into  $dV^\alpha = dV_e^\alpha \left(1 - \frac{V^\alpha}{V}\right)$  we get

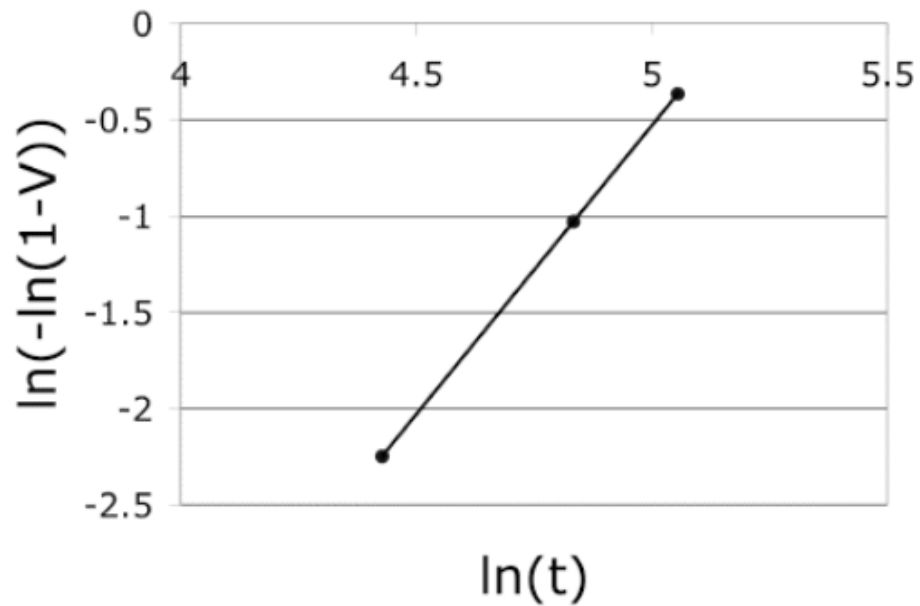
$$dV^\alpha = \left(1 - \frac{V^\alpha}{V}\right) \frac{4}{3}\pi G^3 (t - \tau)^3 I_V V d\tau, \text{ then writing } \xi = V^\alpha / V \text{ and integrating}$$

$$-\ln(1 - \xi) = \frac{4}{3}\pi G^3 I_V \int_0^t (t - \tau)^3 d\tau, \text{ and integrating again}$$

$$\xi = 1 - \exp\{-\pi G^3 I_V t^4 / 3\}$$

[30%]

Using the data in the table provided, a plot of  $\ln\{-\ln(1-\xi)\}$  versus  $\ln(t)$  yields a gradient of 3, as opposed to the above derivation that should produce an exponent of 4. This means that the particles all start from a fixed number of existing nuclei, thus reducing the exponent by one in the integration.



[30%]

7.

Consider the pure components A and B with molar free energies  $\mu_A^0$  and  $\mu_B^0$  respectively. The free energy of a mechanical mixture is simply an average given by:

$$G\{\text{mixture}\} = (1-x)\mu_A^0 + x\mu_B^0$$

where  $x$  is the mole fraction of B. It is assumed that the particles are so large that the A and B atoms do not 'feel' each other's presence via interatomic forces between unlike atoms.

A solid solution is the most intimate mixtures of elementary entities, whether they are atoms or molecules. There will be a reduction in free energy relative to the mechanical mixture, because of the changes in the configurational entropy of mixing. Students may illustrate this using free energy diagrams.

[20%]

The number of A-A bonds in a mole of solution is  $\frac{1}{2}zN_A(1-x)^2$ . This is because in a random solution, the chance of finding an A atom is  $(1-x)$  and that of successively finding two A atoms is therefore  $(1-x)^2$ . The number of B-B bonds is similarly  $\frac{1}{2}zN_Ax^2$ , and number of A-B + B-A bonds is  $zN_A(1-x)x$ .

[20%]

The energy, defined relative to infinitely separated atoms, before mixing is therefore:

$$\frac{1}{2}zN_A \left[ (1-x)(-2\varepsilon_{AA}) + x(-2\varepsilon_{BB}) \right]$$

since the binding energy per pair of atoms is  $-2\varepsilon$  and  $\frac{1}{2}zN_A$  is the number of bonds. After mixing, the corresponding energy is given by:

$$\frac{1}{2}zN_A \left[ (1-x)^2(-2\varepsilon_{AA}) + x^2(-2\varepsilon_{BB}) + 2x(1-x)(-2\varepsilon_{AB}) \right]$$

where the factor of two in the last term is to count A-B and B-A bonds. Therefore, the change in energy due to mixing is the latter minus the former, *i.e.*:

$$\begin{aligned}
\Delta H_M &= -zN_A \left[ (1-x)^2 (\epsilon_{AA}) + x^2 (\epsilon_{BB}) + x(1-x)(2\epsilon_{AB}) - (1-x)(\epsilon_{AA}) - x(\epsilon_{BB}) \right] \\
&= -zN_A \left[ -x(1-x)(\epsilon_{AA}) - x(1-x)(\epsilon_{BB}) + x(1-x)(2\epsilon_{AB}) \right] \\
&= zN_A x(1-x)\omega
\end{aligned}$$

[40%]

It is important to note that this derivation assumes a random distribution of atoms, whereas if  $\Delta H_M \neq 0$  then we do not expect a random distribution at low temperatures.

[10%]

The free energy curve can be made asymmetrical by making the  $\omega$  term a function of concentration.

[10%]